Supporting information

for

Mn, P Co-doped Sharp-edged Mo_2C Nanosheets Anchored on Porous Carbon for Efficient Electrocatalytic Hydrogen Evolution

Zongyun Mu[a, c], Ting Guo[a], Hao Fei[a], Dingsheng Xu[b], Yaoqing Mao[c], Zhuangzhi Wu[a, *], Dezhi Wang[a, *]

[a] *School of Materials Science and Engineering, Central South University, Changsha 410083, China*

[b] *Sinosteel Tianyuan Co. Ltd., Ma'anshan 241000, China*

[c] *Hunan Special Metal Materials Co. Ltd., Changsha 410013, China*

E-mail address: zwu@csu.edu.cn; dzwang@csu.edu.cn

Experiment

Materials

Potassium hypophosphite (KH_2PO_2), phosphomolybdic acid ($H_3O_{40}PMo_{12}$), citric acid ($C_6H_8O_7$), potassium hydroxide (KOH), potassium chloride (KCl) and manganese (II) acetate tetrahydrate ($Mn(CH_3COO)_2 \cdot 4H_2O$) were provided by Shanghai Aladdin Biochemical Technology. Ethanol was purchased from Beijing Chemical Corp. Nafion solution (5 wt%) was obtained from DuPont Company (USA). Sulfuric acid (H_2SO_4, 98%) was provided by Xilong Chemical Co., Ltd. All chemicals were used as received without further treatment.

Synthesis of bulk b-0Mn-Mo_2C and Mn-Mo_2C NS

Typically, for the synthesis of 0.08Mn-Mo_2C NS, 4.2 g citric acid ($C_6H_8O_7$) and 3.36 g KOH were dissolved in 100 mL deionized water and stirred for 1 h to form a transparent solution (marked as solution A). Meanwhile, 0.912 g (0.5 mmol) $H_3O_{40}PMo_{12}$, 3.33 g KH_2PO_2, 10 g KCl and 19.6 mg (0.08 mmol) $Mn(CH_3COO)_2 \cdot 4H_2O$ were mixed by stirring at 90 °C for 1 h to obtain a dark blue solution (marked as solution B). Then, solution B was poured into solution A and kept stirring at 90 °C until the water was completely removed, following by drying at 180 °C for 2 h. Subsequently, the harvested precursor was put downstream in a ceramic boat with 0.025g KH_2PO_2 at the upstream of tube furnace. The system was calcined at 750 °C for 2 h with a heating rate of 7 °C min^{-1} in argon flow, then cooled down naturally to room temperature. Next, the calcined precursor was ground into powder using an agate mortar, then washed with 0.5 M H_2SO_4 and deionized water by ultrasonication for several times. After being dried at 40 °C for 24 h in vacuo, the as-prepared reaction product was collected and denoted as 0.08Mn-Mo_2C NS. According to the different feeding amount of $Mn(CH_3COO)_2 \cdot 4H_2O$ from 0 to 0.5 mmol, the xMn-Mo_2C NS (x=0, 0.01 and 0.16 mmol) products were also synthesized

using the same procedure. Additionally, the bulk Mo_2C without Mn doping (denoted as b-0Mn-Mo_2C) was also obtained by employing the same procedure as 0.08Mn-Mo_2C NS in the absence of KCl and $Mn(CH_3COO)_2 \cdot 4H_2O$.

Synthesis of pure Mo_2C NS

Pure Mo_2C NS without Mn or P doping was synthesized following the same procedure as 0.08Mn-Mo_2C NS excepting that 0.5 mmol $H_3O_{40}PMo_{12}$ was replaced by 0.857 mmol $(NH_4)_6Mo_7O_{24}\cdot 4H_2O$ in the absence of $Mn(CH_3COO)_2 \cdot 4H_2O$ and KH_2PO_2.

Synthesis of Mo_2C NS doped without P dopant

0.08mmol Mn doped Mo_2C NS without P dopant was synthesized following the same procedure as 0.08Mn-Mo_2C NS excepting that 0.5 mmol $H_3O_{40}PMo_{12}$ was replaced by 0.857 mmol $(NH_4)_6Mo_7O_{24}\cdot 4H_2O$ in the absence of KH_2PO_2.

Synthesis of 0.08Mn doped Mo_2C NS prepared with various P addition

0.08mmol Mn doped Mo_2C NS prepared with various P addition was synthesized following the same procedure as 0.08Mn-Mo_2C NS excepting that 3.33 g KH_2PO_2 was replaced by 2.22 g KH_2PO_2 or 4.44 g KH_2PO_2. And the corresponding specimen was marked as 0.08Mn-Mo_2C-2.22 NS and 0.08Mn-Mo_2C-4.44 NS, respectively.

Preparation of working electrodes

The working electrode was prepared in a typical procedure. 3 mg of the measured material was dispersed in a mixture of Nafion solution (5 wt%, 80 μL), ethanol (200 μL) and distilled water (800 μL), and then ultrasonicated for 30 min to get a dark slurry. Afterwards, 5 μL of the slurry was pipetted onto a smooth glass carbon electrode in 3 mm, then dried in air for 5 h. The mass loading of the catalyst was calculated to be 0.213 mg cm^{-2}.

Characterizations

The X-ray diffraction (XRD) patterns were collected by D/max 2500 X-ray diffractometer using a Cu Kα radiation. The morphology and microstructure were observed using FEI Sirion 200 scanning electron microscopy (SEM) and JEOL 2100F transmission electron microscope (TEM) equipped with quantitative X-ray spectroscopy capabilities for element distribution analysis. The surface compositions and element chemical states were detected by X-ray photoelectron spectroscopy (XPS, Thermo Fisher Scientific K-ALPHA) with an Al Ka radiation using C 1s (284.6 eV) as a reference. Brunauer-Emmett-Telle (BET) surface area and the pore size distribution were acquired on Quadrasorb SI-3MP with nitrogen adsorption at 77 K. The Mn and P content was determined by inductively coupled plasma (ICP-OES, Agilent 725).

Electrochemical measurements

The electrochemical experiments were conducted on an electrochemical workstation (CHI 660E) with a three-electrode system in 0.5 M H_2SO_4. The saturated calomel electrode (SCE), the as-prepared glassy carbon electrode and the graphite rod were used as the reference electrode, working electrode and counter electrode, respectively. To assess the activity, the linear sweep voltammograms were adopted in the range from 0.1 V to 0.4V at 2 mV s^{-1}. Electrochemical impedance spectroscopy (EIS) was applied from 1 MHz to 1 Hz with an amplitude of 5 mV at an overpotential of 0.2 V. The cyclic voltammetry (CV) curves were obtained from 0 to 0.3 V at various scan rates (20, 40, 60, 80, 100, 120 and 140 mV s^{-1}) to deduce the electrochemical double-layer capacitances (C_{dl}) and electrochemically active surface area (ECSA). The slopes k of the fitting line from current density variation plotted against scan rate curves were obtained, and $C_{dl} = k/2$.

The ECSA was calculated according to the following formula[1]:

$$A_{ECSA} = \frac{\text{electrochemical capacitance}}{40\ \mu F\ cm^{-2}\ per\ cm^{2}_{ECSA}}$$

The turnover frequency (TOF) can be calculated by the formula below:

$$TOF = \frac{\text{no. of total hydrogen turnovers } cm^{-2} \text{ of geometric area}}{\text{no. of active sites } cm^{-2} \text{ of geometric area}}$$

The total number of hydrogen turnovers per current density can be calculated using the formula:

$$\text{No. of } H_2 = (\text{per } \frac{mA}{cm^2})(\frac{1\ C\ s^{-1}}{1000\ mA})(\frac{1 \text{ mol of e}}{96485.3\ C})(\frac{1 \text{ mol of } H_2}{2 \text{ mol of e}})(\frac{6.022 \times 10^{23} H_2 \text{ molecules}}{1 \text{ mol of } H_2})$$

$$= 3.12\times10^{15}\ \frac{H_2\ s^{-1}}{cm^2}\ \text{per}\ \frac{mA}{cm^2}$$

Due to the uncertainty of real hydrogen adsorption site, the number of active sites was evaluated from the surface sites, where Mo and C atoms act as possible active sites. On the basis of roughness factor and the unit cell of Mo_2C (volume of 37.2 $Å^3$), the number of active sites per real surface area is given by the following formula:

$$no.\ of\ active\ sites = \left(\frac{2\frac{atoms}{unit\ cell}}{37.2\frac{Å^3}{unit\ cell}}\right)^{2/3} = 1.42 \times 10^{15}\ atoms\ cm_{real}{}^{-2}$$

Finally, plots of the current density can be converted into TOF plots according to:

$$TOF = \frac{\left(3.12 \times 10^{15}\frac{H_2/s}{cm^2}\ per\ \frac{mA}{cm^2} \times |j|\right)}{\left(1.42 \times 10^{15}\ atoms\ cm_{real}{}^{-2}\right)A_{ECSA}}$$

The long-term stability of the catalysts was assessed by continuous CV scanning and chronoamperometry. All the potentials reported in this work were referenced to a reversible hydrogen electrode based on the Nernst equation ($E_{RHE} = E_{SCE} + 0.059*pH + 0.209$) without iR corrections.

Computational details

The density functional theory (DFT) calculations were conducted using VASP (Vienna ab initio simulation package) within the projector-augmented plane wave pseudopotentials to process the ion-electron interactions. The electronic exchange and correlation effects were modeled by the Perdew-Burke-Ernzerhof (PBE) of Generalized Gradient Approximation (GGA). The model of β-Mo_2C was constructed based on Wang's work[2]. A periodic 4 × 4 × 1 supercell with a Γ-centered 2 × 2 × 1 k-point grid was used to conduct the surface analysis and calculation in Brillouin zone. A cutoff energy of 520 eV was set for the plane-wave basis. The Mo_2C (001) surface was established to calculate the Gibbs free energy of hydrogen adsorption (ΔG_{H*}), where 15 Å vacuum above the surface was taken into consideration. ΔG_{H*} was calculated using the following equation:

$$\Delta G = E_{total}-E_{surface}-1/2E_{H2}+ \Delta E_{ZPE} - T\Delta S$$

where E_{total}, $E_{surface}$, E_{H2}, ΔE_{ZPE} and ΔS were referred to total energy for the surface with H adsorption, the surface without H adsorption, the energy of H_2 in gas phase, the zero-point energy change and the entropy change, respectively. In vaspkit 501 function mode, ΔE_{ZPE} and ΔS were calculated as G(T) on account of frequency calculation. Finally, in reference of the investigation form Nørskov, ΔG_{H*} was calculated as follows:

$$\Delta G_{H*}=\Delta E_{H*} + 0.24 \text{ eV}$$

where $\Delta E_{H*} = E_{total}-E_{surface}-1/2E_{H2}$.

Table S1 The calculated lattice constants and grain sizes of samples.

Sample	Grain size / nm	Lattice constant / Å		
		a	*b*	*c*
0Mn-Mo_2C NS	22.7	3.0168	3.0168	4.7401
0.01Mn- Mo_2C NS	21.3	3.0137	3.0137	4.7391
0.08Mn- Mo_2C NS	21.2	3.0104	3.0104	4.7366
0.16Mn- Mo_2C NS	21.0	3.0040	3.0040	4.7360

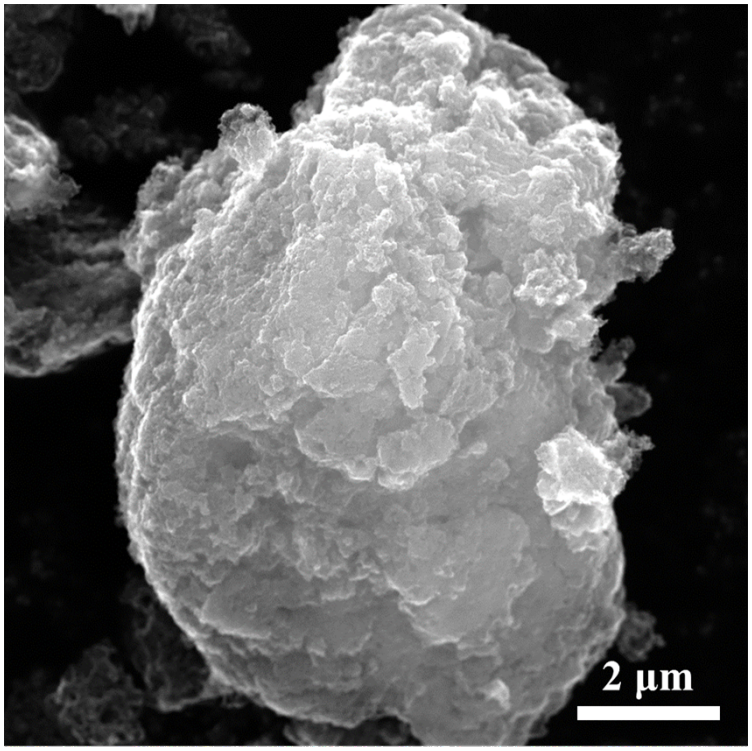

Fig. S1 SEM image of b-0Mn-Mo_2C.

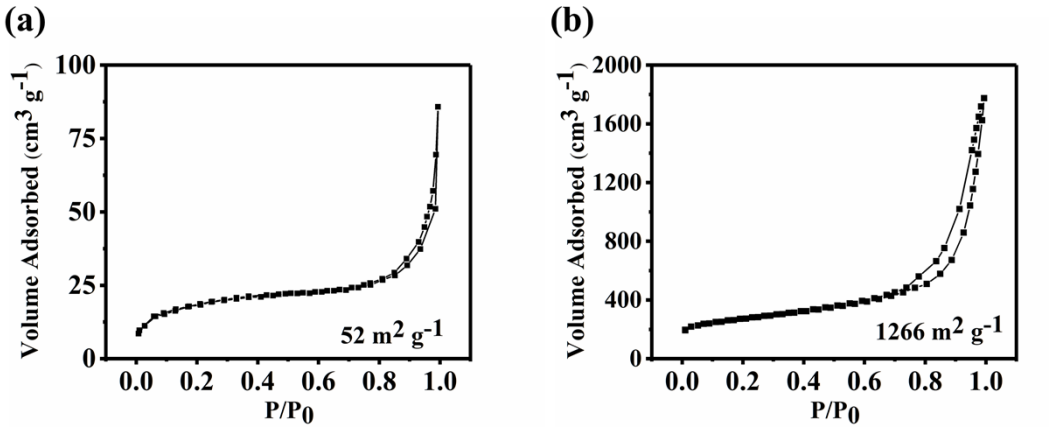

Fig. S2 Nitrogen adsorption–desorption isotherms of (a) b-0Mn-Mo_2C and (b) 0.08Mn-Mo_2C NS.

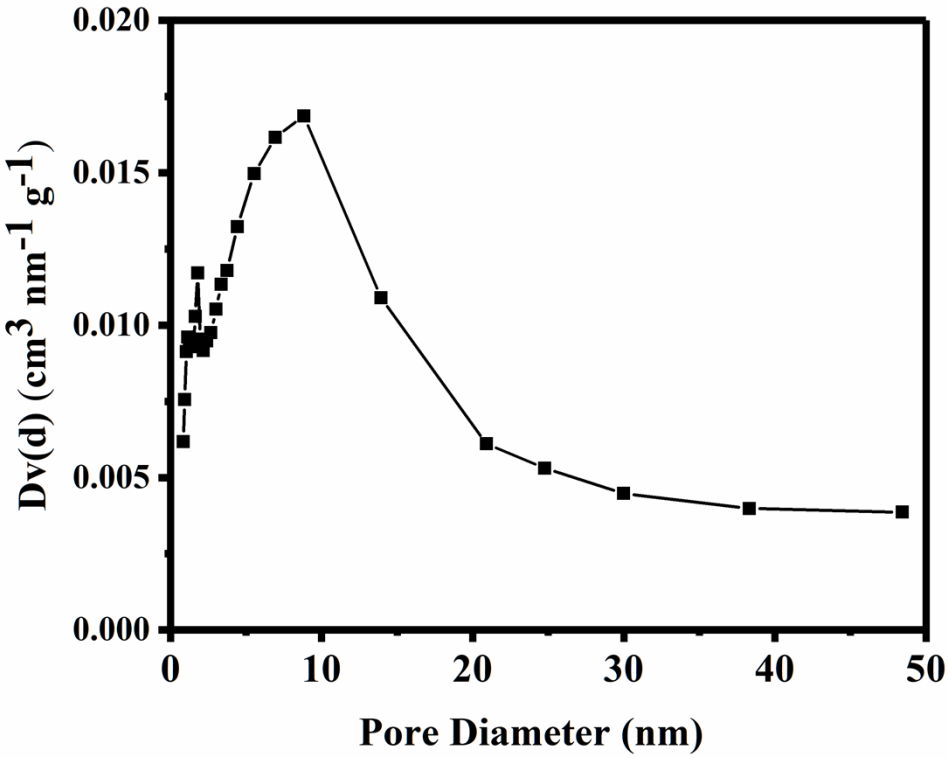

Fig. S3 Pore size distribution curve of 0.08Mn-Mo_2C NS.

Table S2 Mn contents of various electrocatalysts measured by ICP.

Sample	Mn wt%
0Mn-Mo_2C NS	0
0.01Mn- Mo_2C NS	0.08
0.08Mn- Mo_2C NS	0.69
0.16Mn- Mo_2C NS	1.38

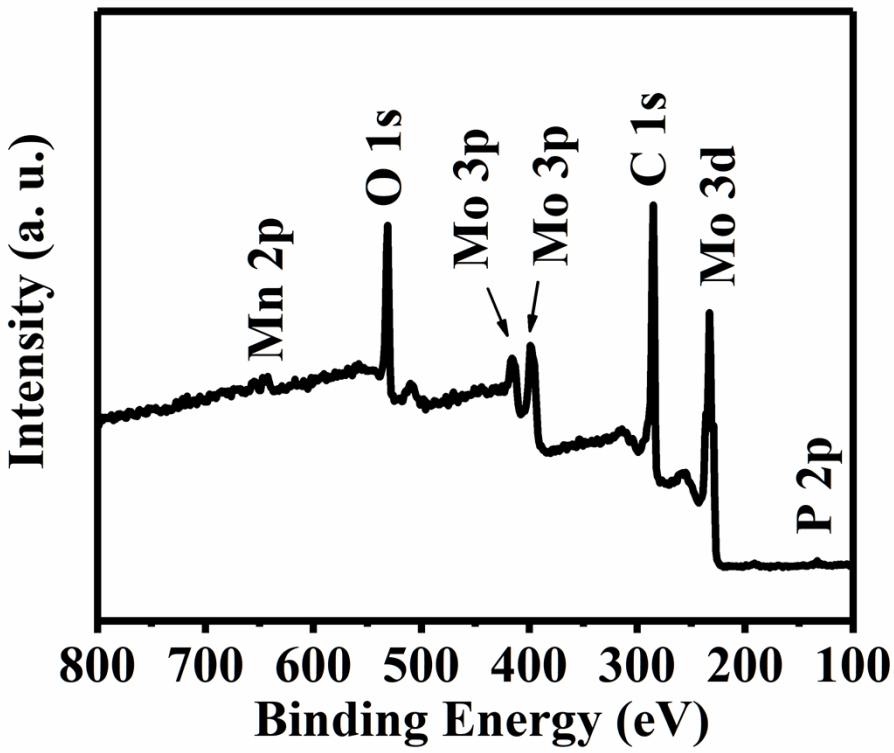

Fig. S4 XPS survey of 0.08Mn-Mo_2C NS.

Table S3 Comparison of the electrocatalytic activity over 0.08Mn-Mo_2C NS with other related electrocatalysts for HER in 0.5 M H_2SO_4.

Catalysts	Loading (mg cm^{-2})	Current density j (mA cm^{-2})	Overpotential at the corresponding j (mV)	Tafel slope (mV dec^{-1})	Ref
Mn, N-Mo_2C-0.01	~0.55	10	-163	66	[3]
Mo_2N-Mo_2C/HGr-3	~0.337	10	-157	55	[4]
Mo_2C/CNT-GR	~0.65	10	-130	58	[5]
Mo-Mo_2C-0.077	~0.38	10	-150	55	[6]
Mo_2C-GNR	/	10	-152	65	[7]
Co-Mo_2C-0.020	0.14	10	-140	39	[8]
Co-NC@Mo_2C	~0.83	10	-143	60	[9]
Mo_2C@NC	0.5	10	-36	33.7	[10]
uf-Mo_2C/CF-2	0.25	10	-184	71	[11]
Mo_2C/C (2:2)	0.28	10	-180	71	[12]
P-Mo_2C@C	1.3	10	-89	42	[13]
N, P-Mo_2C@C	0.9	10	-141	56	[14]
Biochar-derived Mo_2C	0.213	10	-161	57	[15]
Mn, P co-doped 0.08Mn-Mo_2C NS	0.213	10	-180	52	This work

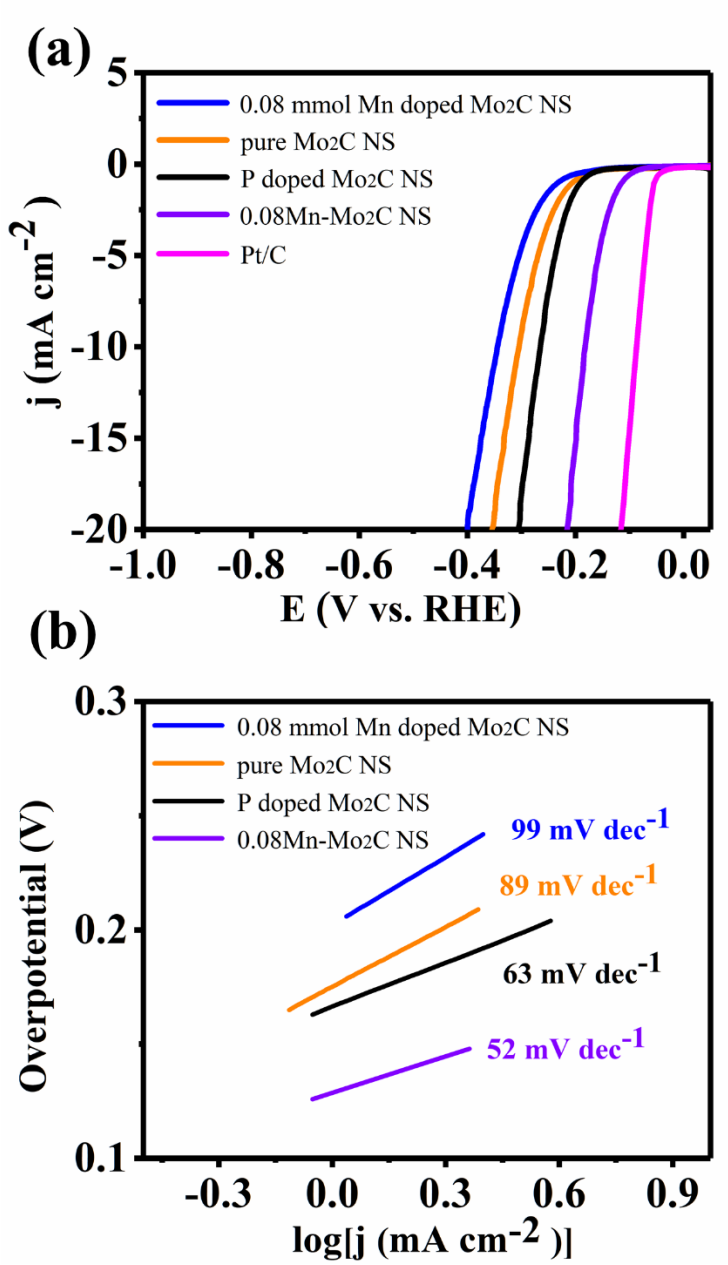

Fig. S5 Electrochemical performances of various samples in 0.5 M H_2SO_4: (a) Polarization curves; (b) Tafel plots.

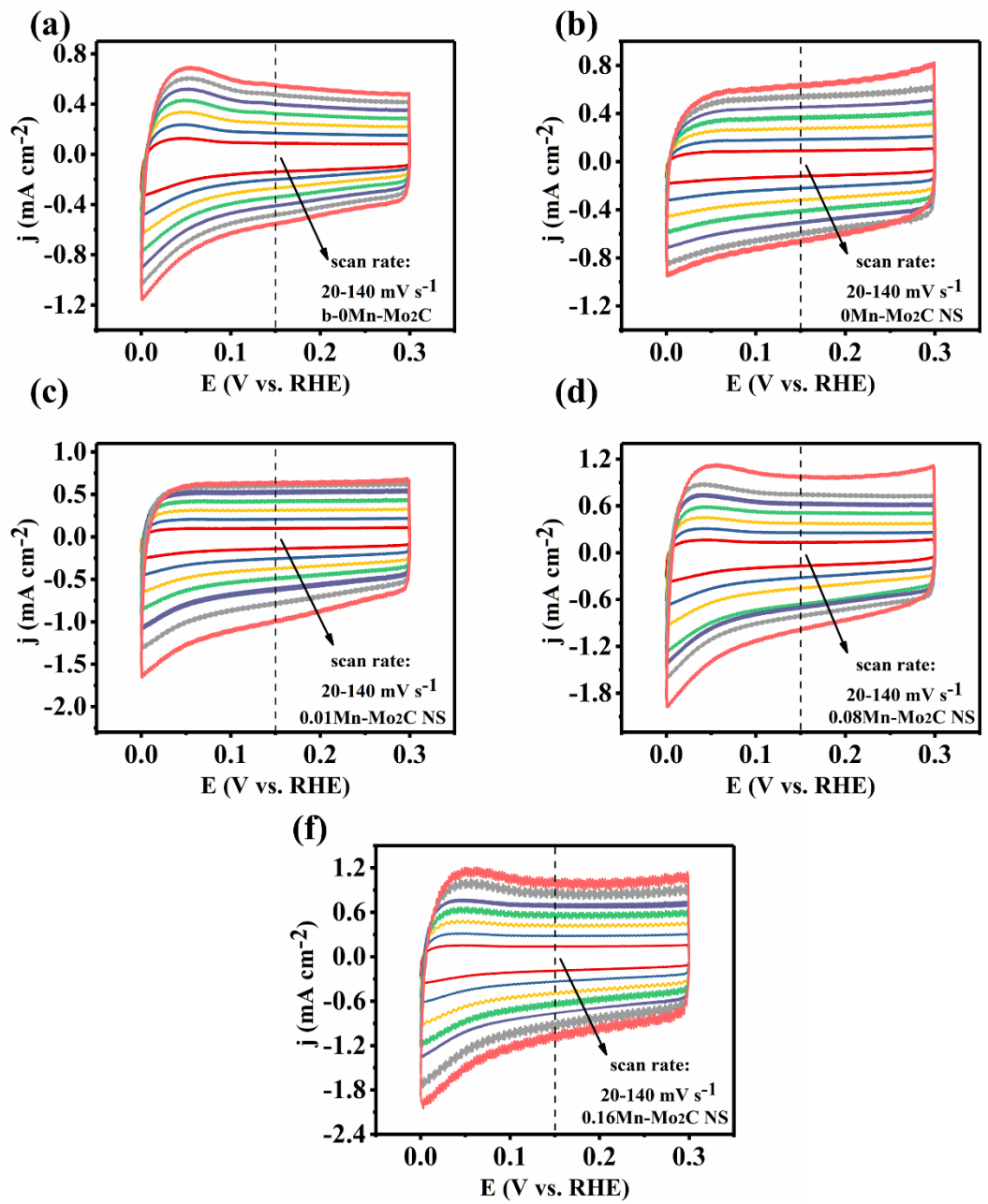

Fig. S6 Electrochemical capacitance measurements in 0.5 M H_2SO_4: (a) b-0Mn-Mo_2C; (b) 0Mn-Mo_2C NS; (c) 0.01Mn-Mo_2C NS; (d) 0.08Mn-Mo_2C NS and (e) 0.16Mn-Mo_2C NS.

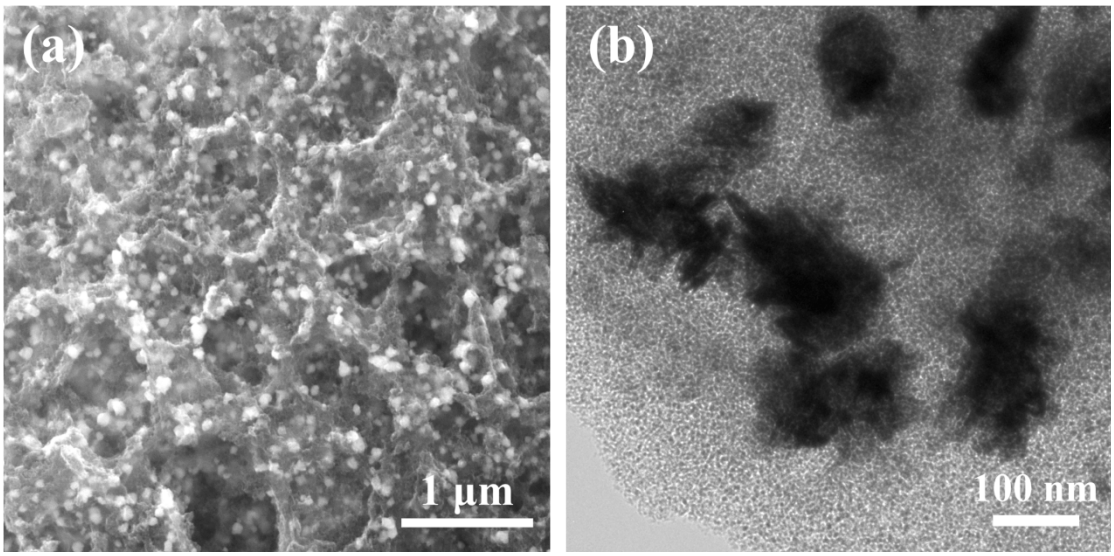

Fig. S7 (a) SEM and (b) TEM images of the morphology and structure of 0.08Mn-Mo_2C NS after long-time stability test.

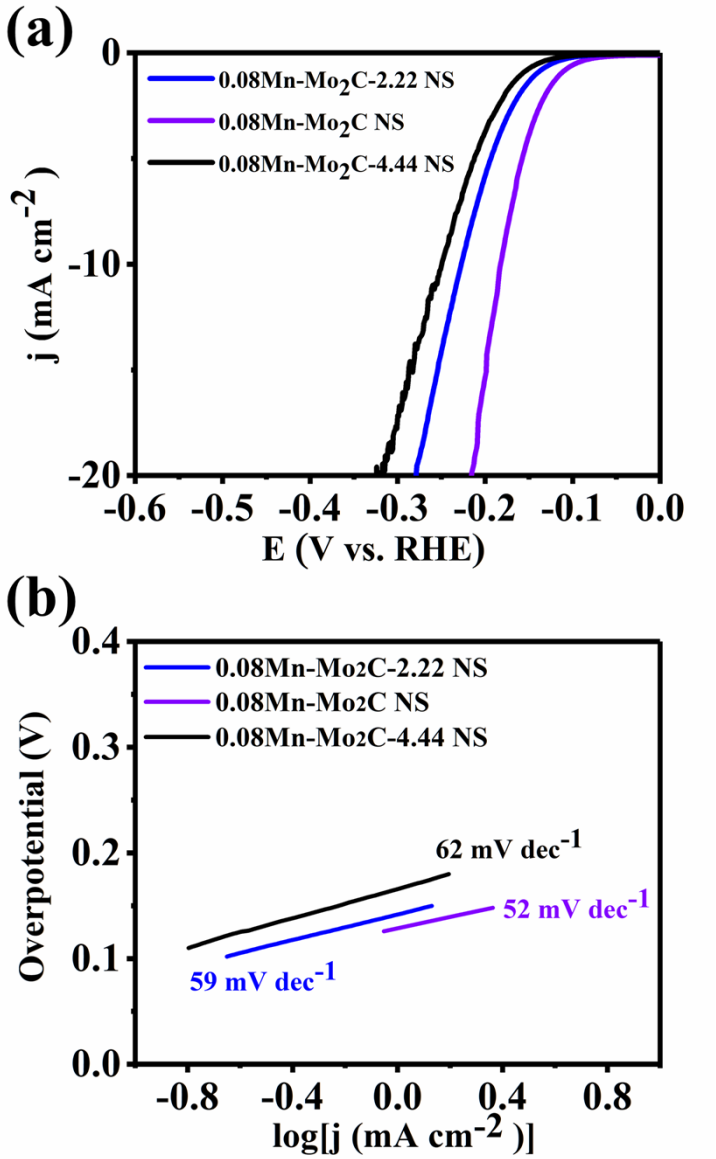

Fig. S8 (a) LSV and (b) Tafel slope of 0.08Mn doped Mo_2C NS prepared with various P addition

Table S4 The P content in 0.08Mn doped Mo_2C NS prepared with various P addition.

Sample	P wt%
0.08Mn-Mo_2C-2.22 NS	0.9
0.08Mn-Mo_2C NS	1.8
0.08Mn-Mo_2C-4.44 NS	2.9

Table S5 The calculated Gibbs free energies (ΔG_{H*}) for H adsorption on the different active sites in each atomic model and the corresponding HER performance.

Model	The corresponding catalyst in the work	Active site	$\triangle G_{H*}$ eV	Tafel mV dec^{-1}	Overpotential at Current density Of 10 mA cm^{-2}
pure Mo_2C	pure Mo_2C NS	Mo site	-0.1865	89	-305
P doped Mo_2C	0Mn-Mo_2C NS	Mo site	-0.1212	63	-264
		P site	0.1143		
Mn doped Mo_2C	0.08 mmol Mn doped Mo_2C NS	Mo site	-0.4075	99	-345
		Mn site	-0.4446		
Mn, P co-doped Mo_2C	0.08Mn-Mo_2C NS	Mo site	-0.0643	52	-180
		Mn site	-0.0094		
		P site	-0.0269		

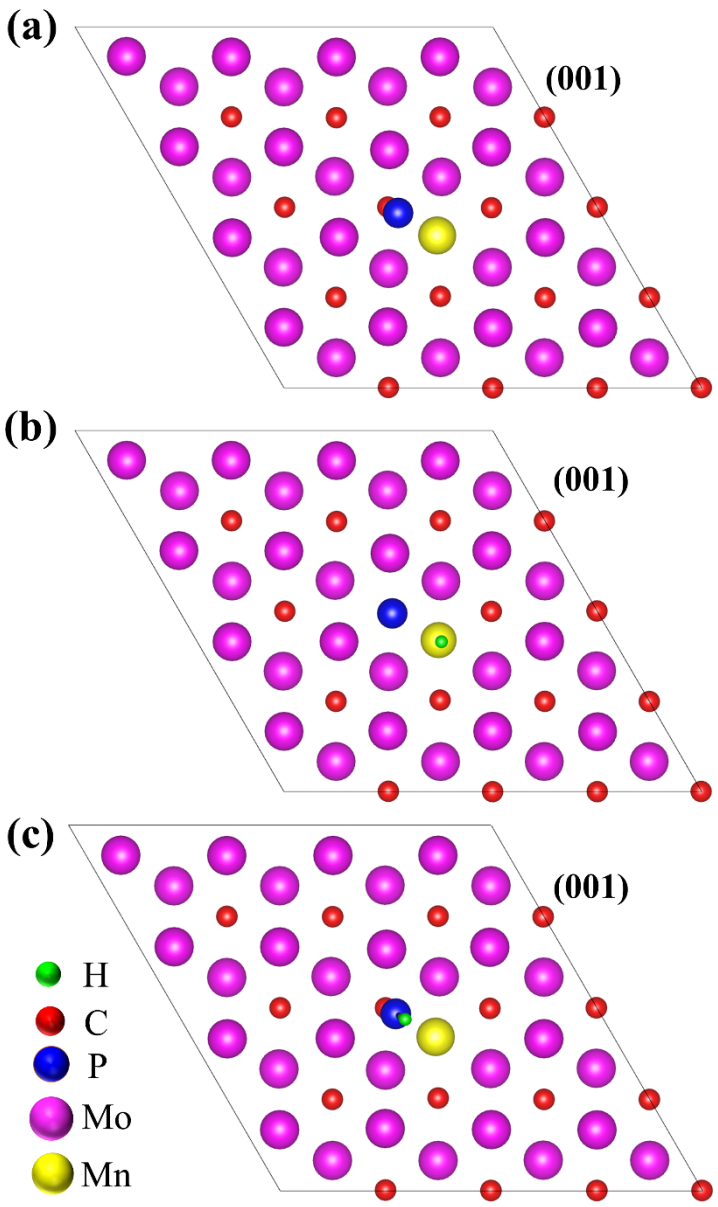

Fig. S9 (a) Theoretical structural models of Mn, P co-doped Mo_2C; Corresponding adsorption of H* on (b) Mn site and (c) P site.

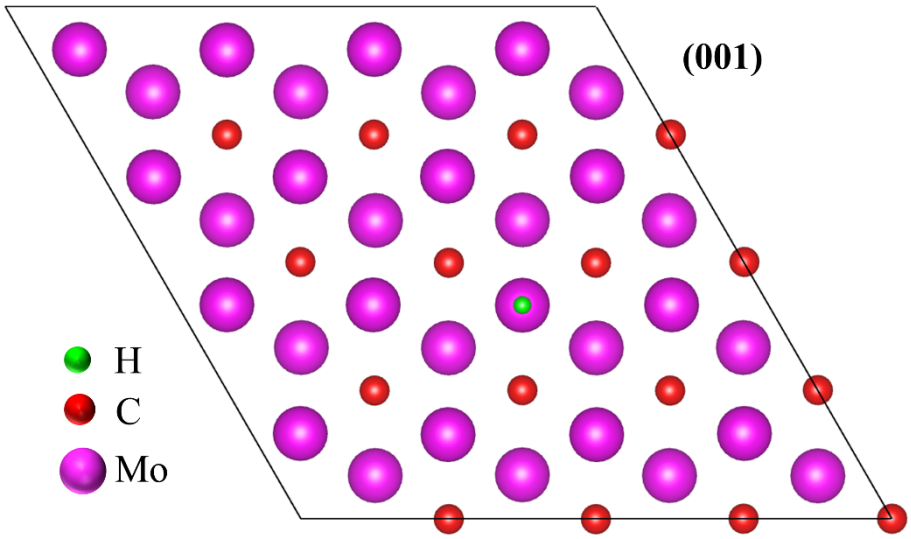

Fig. S10 Theoretical structural models of pure Mo_2C with the most stable adsorption of H* on Mo site.

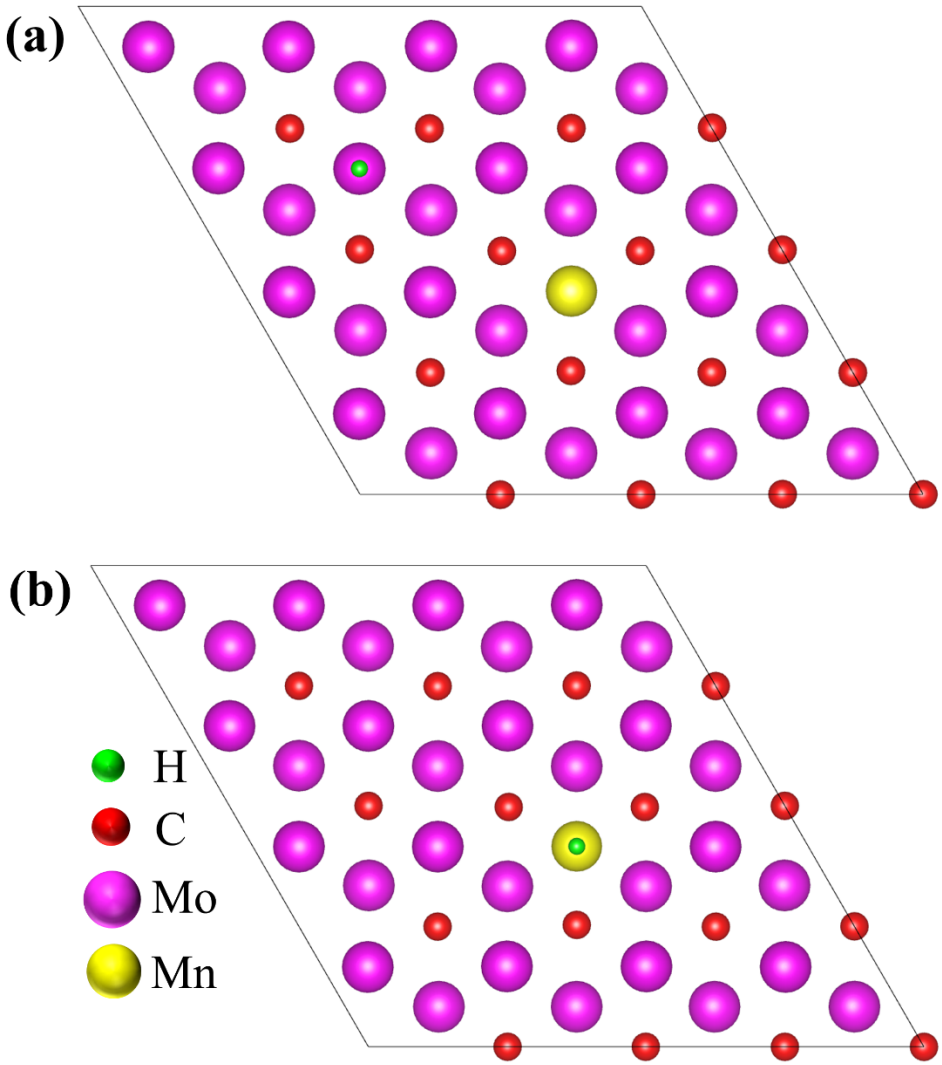

Fig. S11 Theoretical structural models of Mn doped Mo_2C with the most stable adsorption of H* on (a) Mo site and (b) Mn site.

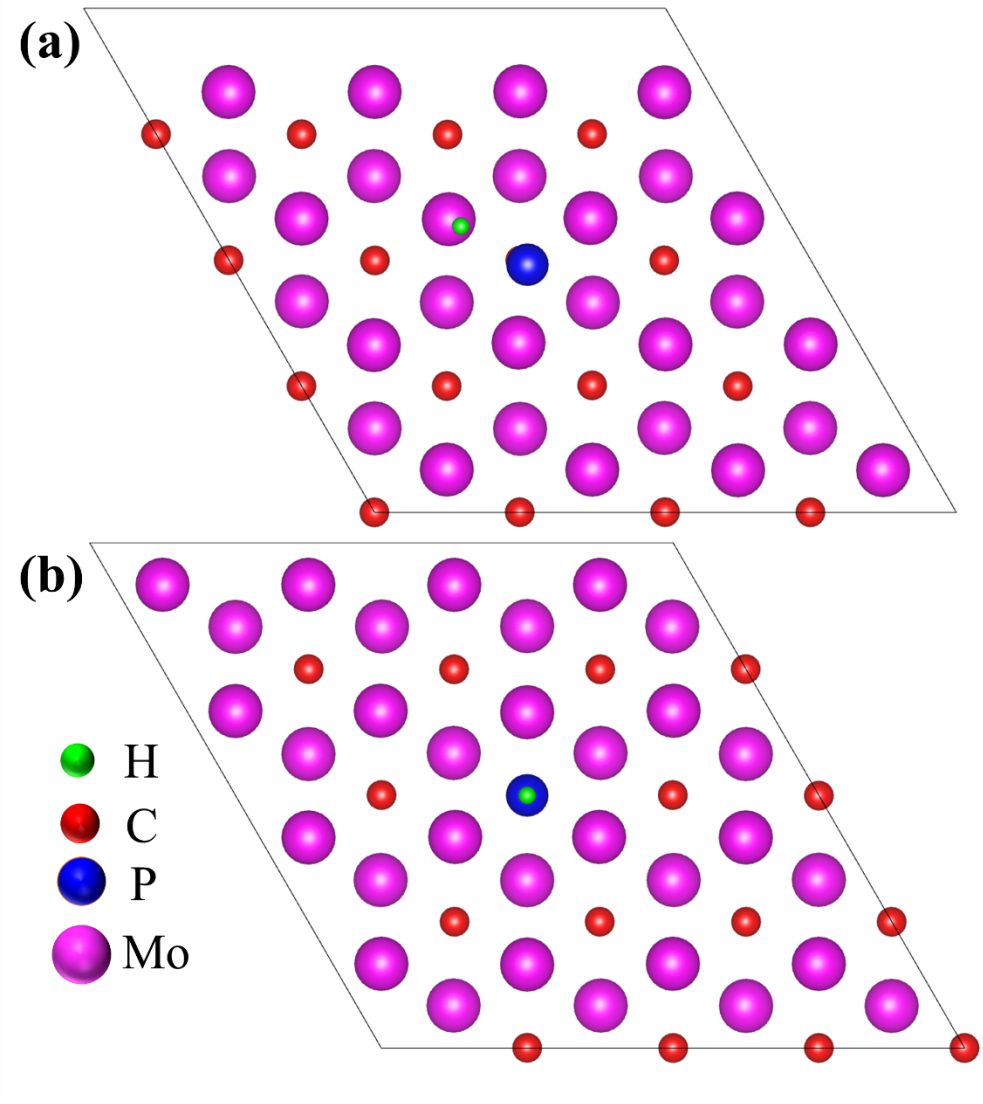

Fig. S12 Theoretical structural models of P doped Mo_2C with the most stable adsorption of H* on (a) Mo site and (b) P site.

References

1 J. Kibsgaard and T. F. Jaramillo, *Angew. Chemie Int. Ed.*, 2014, **53**, 14433–14437.

2 T. Wang, X. Liu, S. Wang, C. Huo, Y.-W. Li, J. Wang and H. Jiao, *J. Phys. Chem. C*, 2011, **115**, 22360–22368.

3 Y. Zhou, J. Xu, C. Lian, L. Ge, L. Zhang, L. Li, Y. Li, M. Wang, H. Liu and Y. Li, *Inorg. Chem. Front.*, 2019, **6**, 2464–2471.

4 H. Yan, Y. Xie, Y. Jiao, A. Wu, C. Tian, X. Zhang, L. Wang and H. Fu, *Adv. Mater.*, 2018, **30**, 1704156–1704163.

5 D. H. Youn, S. Han, J. Y. Kim, J. Y. Kim, H. Park, S. H. Choi and J. S. Lee, *ACS Nano*, 2014, **8**, 5164–5173.

6 J. Dong, Q. Wu, C. Huang, W. Yao and Q. Xu, *J. Mater. Chem. A*, 2018, **6**, 10028–10035.

7 X. Fan, Y. Liu, Z. Peng, Z. Zhang, H. Zhou, X. Zhang, B. I. Yakobson, W. A. Goddard, X. Guo, R. H. Hauge and J. M. Tour, *ACS Nano*, 2017, **11**, 384–394.

8 H. Lin, N. Liu, Z. Shi, Y. Guo, Y. Tang and Q. Gao, *Adv. Funct. Mater.*, 2016, **26**, 5590–5598.

9 Q. Liang, H. Jin, Z. Wang, Y. Xiong, S. Yuan, X. Zeng, D. He and S. Mu, *Nano Energy*, 2019, **57**, 746–752.

10 Z. Cheng, Q. Fu, Q. Han, Y. Xiao, Y. Liang, Y. Zhao and L. Qu, *Adv. Funct. Mater.*, 2018, **28**, 1705967–1705974.

11 Z. Kou, T. Wang, Y. Cai, C. Guan, Z. Pu, C. Zhu, Y. Hu, A. M. Elshahawy, J. Wang and S. Mu, *Small Methods*, 2018, **2**, 1700396–1700402.

12 C. Wu and J. Li, *ACS Appl. Mater. Interfaces*, 2017, **9**, 41314–41322.

13 Z. Shi, K. Nie, Z.-J. Shao, B. Gao, H. Lin, H. Zhang, B. Liu, Y. Wang, Y. Zhang, X. Sun, X.-M.

Cao, P. Hu, Q. Gao and Y. Tang, *Energy Environ. Sci.*, 2017, **10**, 1262–1271.

14 Y.-Y. Chen, Y. Zhang, W.-J. Jiang, X. Zhang, Z. Dai, L.-J. Wan and J.-S. Hu, *ACS Nano*, 2016, **10**, 8851–8860.

15 T. Guo, X. Zhang, T. Liu, Z. Wu and D. Wang, *Appl. Surf. Sci.*, 2020, **509**, 144879–144886.